

Optically induced metastable paramagnetic states in amorphous semiconductors

S. G. Bishop, U. Strom, and P. C. Taylor
Naval Research Laboratory, Washington, D. C. 20375
 (Received 20 October 1976)

Mid-gap optical absorption and electron spin resonance (ESR) attributed to optically induced localized paramagnetic states have been studied in several chalcogenide glasses and amorphous arsenic for $T \leq 80$ K. The observation of these optically induced metastable paramagnetic centers provides the most direct evidence yet obtained for the existence of localized gap states in these amorphous semiconductors. Irradiation with light whose energy corresponds to the Urbach tail of the absorption edge ($\alpha \simeq 100 \text{ cm}^{-1}$) excites photoluminescence (PL) which fatigues (decays) with continuing excitation. The fatigue of the PL is accompanied by the appearance of a growing ESR signal which is not present before illumination. The occurrence of an associated induced optical absorption demonstrates that the paramagnetic states are located in the forbidden gap of these amorphous semiconductors. Subsequent prolonged irradiation of the sample with infrared light in the mid-gap induced absorption band reduces the strength of or "bleaches" both the optically induced ESR signal and the induced absorption and restores the fatigued PL to its cold dark (initial) efficiency. These facts suggest a mechanism whereby radiative recombination centers which become inactive during PL fatigue are closely associated with the production of the metastable paramagnetic centers. The optically induced ESR centers are apparently unique to the amorphous phase and their density (N_s) saturates at or below 10^{17} spins per cm^3 in all materials measured to date regardless of light intensity. Analysis of the ESR spectra has led to the identification of a hole center which consists of an electron missing from a nonbonding lone pair chalcogen orbital and a center in As-containing glasses and amorphous arsenic which is localized in an As p orbital. A detailed account of the ESR spectral analysis is presented. Changes in the local structural order as a function of composition appear as changes in the g values and width of the optically induced ESR spectrum. The value of N_s is also a function of composition with the highest values occurring in glasses containing substantial amounts of As such as As_2Se_3 . The addition of Ge depresses N_s to levels as low as $\sim 5 \times 10^{15} \text{ cm}^{-3}$ in GeSe_2 , indicating that the structural differences which accompany the introduction of tetrahedrally coordinated Ge reduce the density of the specific structural anomaly which determines the value of N_s . Possible mechanisms for the generation of the optically induced states are presented, and the relationship between the experimental results and various models proposed to explain the properties of localized gap states is discussed.

I. INTRODUCTION

Localized gap states have figured prominently in the phenomenological models proposed to describe the distribution of electronic states in amorphous semiconductors¹⁻⁴ and in the interpretation of various transport,^{5,6} optical absorption,⁷ photoconductivity,⁴ and photoluminescence⁸⁻¹² experiments carried out on these materials. Both the diversity of models proposed to date and the apparently contradictory results or interpretations of various experiments attest to the wide range of prevailing opinions concerning the concentration, distribution, and origin of such localized states in the gap of amorphous semiconductors. Perhaps the most persistent example of contradictory experimental results has been the observation by electron spin resonance (ESR) techniques¹³ that the number of unpaired spins in chalcogenide glasses ($< 10^{14} \text{ cm}^{-3}$) is far below the number expected on the basis of the density of localized states at the Fermi energy, $g(E_F)$, obtained from ac conductivity^{5,6,14} and field-effect¹⁵ experiments. The failure to observe Curie paramagnetism at low temperatures provides further evi-

dence of the diamagnetism of pure chalcogenide glasses.¹⁶ One is faced with the conceptual problem of pinning the Fermi energy in the gap with localized states without producing detectable numbers of unpaired spins.

It can be argued that most of the localized states are doubly occupied and therefore not paramagnetic,^{5,7,13,17} and that the density of any unpaired electrons near the Fermi level is too small to be observable. Anderson,¹⁷ Mott, Davis, and Street,^{18,19} and Economou, Reinecke, and Ngai²⁰ have recently proposed models which explain the diamagnetism of chalcogenide glasses in terms of such two-electron states which are all either doubly occupied or empty. For this case it should be possible to disturb the diamagnetic equilibrium distribution of electrons by optically injecting electron-hole pairs and thereby producing a detectable density of unpaired spins. Recently we reported the first observation of optically induced localized paramagnetic states in the forbidden gap of chalcogenide glasses and amorphous arsenic.²¹⁻²³ It was found that low-temperature irradiation of chalcogenide glasses such as Se, As_2Se_3 , and As_2S_3 with photon energies corresponding to the

Urbach tail in the absorption edge (absorption coefficient $\sim 100 \text{ cm}^{-1}$) produces an ESR which is not present in the equilibrium cold-dark (unirradiated) state. An associated induced mid-gap optical absorption demonstrates that the paramagnetic states are located in the forbidden gap of these glasses. On the basis of the ESR spectra it was concluded that the optically induced paramagnetic centers are localized on major constituent atoms (arsenic and chalcogen atoms) rather than on chemical impurities and can in this respect be regarded as an intrinsic property of these glasses.

These results have constituted what is perhaps the most direct experimental observation of localized states in the gap of chalcogenide glasses. While the induced paramagnetic states represent a nonequilibrium condition in the glass, the fact that they are metastable at low temperatures and are localized on major constituent atoms allows them to be used as highly sensitive probes of the local structural environment. The ESR spectra convey information concerning the bonding configuration and localization of the paramagnetic centers as well as restrictions on the possible percentage of these optically induced localized states.

In this paper the results of experimental studies of optically induced localized paramagnetic states in a variety of chalcogenide glasses and amorphous arsenic are presented. Unsuccessful attempts to observe these effects in crystalline chalcogenides and amorphous Ge and Si are also mentioned briefly. After discussion of the experimental methods and presentation of the optical and ESR data, a detailed account of the methods employed to analyze the ESR spectra is given along with the conclusions to be drawn from the results of this analysis. Finally, possible mechanisms for the generation of the optically induced states are presented, and the restrictions which the experimental results place upon the models proposed to explain the nature of localized gap states are discussed.

II. EXPERIMENTAL PROCEDURE

Earlier attempts to detect or study paramagnetism due to intrinsic localized states in chalcogenide glasses using ESR or magnetic susceptibility techniques were hampered by the presence of trace amounts of paramagnetic impurities such as Fe.¹⁶ The experiments discussed here circumvent these difficulties by focusing on optically induced paramagnetic centers alone. Most of the samples studied exhibited some ESR signal in the cold dark, i.e., before irradiation. However, so long as the signals were weak, did not occur near

the free-electron g value, and were unaffected by optical excitation, these cold-dark spectra could be distinguished accurately from the signals due to the optically induced metastable gap states. Furthermore, none of the optically induced ESR centers studied displayed spin-Hamiltonian parameters (hyperfine constants or g values) which were consistent with localization on impurity atoms. All centers appear to be localized on major constituent atoms (chalcogens, As or Ge).

Nevertheless, reliable observation of the optically induced paramagnetism requires a high degree of sample purity. Samples of glassy As_2Se_3 , $\text{As}_2\text{Se}_{1.5}\text{Te}_{1.5}$, As_2S_3 , GeSe_2 , and several more complicated compositions were prepared from 99.999%-pure elemental constituents in sealed quartz ampoules by standard rocking furnace techniques followed by an air quench. Pure Se was obtained from Atomergic Inc., and standard optical flats of As_2S_3 doped with ~ 1000 -ppm Sb and known to contain traces of Fe were obtained from Servo, Inc. As expected, all of these samples exhibited some weak broad ESR in the cold dark (4.2 K) due to the presence of paramagnetic impurities, but the samples singled out for detailed study exhibited no sharply defined spectral features in the ESR derivative spectrum in the vicinity of $g=2$ ($1.5 \leq g \leq 3.0$). In addition, a high purity, strain relieved (annealed) sample of glassy As_2Se_3 was obtained from Alfred University and no cold-dark ESR signal was observed in this sample under the operating conditions employed in the observation of the optically induced ESR. A signal was observed near $g \approx 4.3$ from the quartz sample tube.

The ESR spectra were obtained at 4.2 K in a helium gas flow variable temperature Dewar system with a standard Varian E-9 X-band (9 GHz) bridge spectrometer, and an optical access cavity. The spectrometer was operated in conjunction with a signal averaging system which facilitated the subtraction of background resonances from the optically induced signals. In the usual procedure, ESR spectra were first obtained in the cold dark and the sample was then irradiated in the cavity with light having photon energy which corresponds to a band edge absorption coefficient of about 100 cm^{-1} . Such light also excites luminescence which fatigues and produces the optically induced mid-gap absorption. In the chalcogenide glasses studied, irradiation of the cold sample in the cavity for a few minutes with approximately 1 mW/cm^2 of the prescribed interband wavelength produced a clearly observable ESR spectrum near $g=2$ which was not present in the cold dark. Usually, irradiation for 1 min was sufficient to produce an observable resonance, but the ESR intensity continued to grow

with longer exposure until it approached a saturated level with an average generation time constant of approximately 10 min for light whose penetration depth was $\sim 100 \mu\text{m}$. Longer saturation times were observed for less absorbed light. These induced centers could subsequently be optically bleached or quenched using light within the band gap as described below.

The number of optically induced spins was determined in each case by comparison of the suitably normalized integrated intensity of the saturated optically induced ESR spectrum with the intensity of the ESR spectrum obtained from a standard sample containing a known number of spins. Densities of optically induced spins were then calculated using estimates of the active sample volume obtained from knowledge of the penetration depth of the inducing light.

Optically induced absorption experiments were carried out as follows. Hot pressed or polished platelets of glass 100 to 500 μm thick were cooled to 80 or 6 K on an optical cold finger Dewar. Light from a tungsten source was first passed through a series of neutral density filters and a monochromator, mechanically chopped at 70 Hz, and then transmitted through the sample ($\leq 0.01\text{-mW/cm}^2$ intensity) and detected by a PbS photoconductive cell and a lock-in amplifier. The transmission of the samples was measured from the band edge out to about 0.4 eV, in which range these glasses are rather transparent with $\alpha \leq 1 \text{ cm}^{-1}$. The source monochromator was then set to a wavelength corresponding to the onset of the absorption edge or Urbach tail ($\alpha \cong 100 \text{ cm}^{-1}$) which characterizes the chalcogenide glasses.⁷ The neutral density filters were removed and the sample was irradiated (to a depth of $\sim 100 \mu\text{m}$) with this band-gap light having intensity $\sim 1 \text{ mW/cm}^2$ which was greater by two orders of magnitude than that with which the transmission was measured. After an irradiation of a few minutes duration, the neutral density filters were reinserted, and the sample transmission was again measured from the band edge to 0.4 eV with the low-level light intensity. After inducing and measuring the absorption below the band edge in this fashion, bleaching or optical quenching experiments could then be carried out in which the optically induced mid-gap absorption is reduced in strength by irradiation with $\sim 1 \text{ mW/cm}^2$ of light in the induced absorption band.

III. EXPERIMENTAL RESULTS

A. Optically induced ESR spectra

The optically induced ESR spectra obtained in glassy Se, As_2Se_3 , and As_2S_3 are shown in Fig. 1,

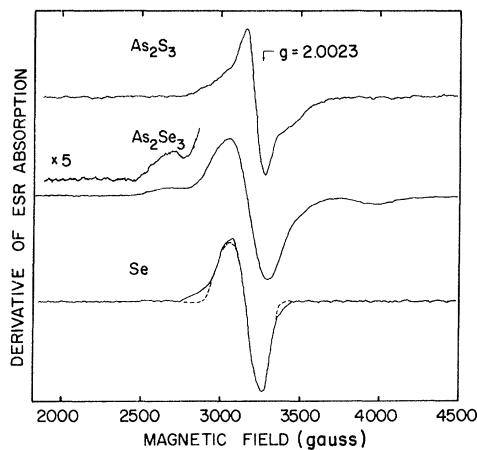


FIG. 1. Optically induced ESR spectra obtained near 4.2 K in chalcogenide glasses. Dashed line superimposed in Se curve is a computer simulation.

and the photon energies which were used to induce them are listed in Table I. We have shown previously²¹ that the most efficient production of metastable ESR centers occurs for photon energies which correspond to absorption coefficients $\alpha \sim 100 \text{ cm}^{-1}$. However, better ESR signals can be obtained²² through the use of more intense laser sources which penetrate $\sim 1 \text{ mm}$. For example, the ESR spectrum of Fig. 1 for glassy Se was induced with the 6328- \AA line of a He-Ne gas laser, and the spectrum for glassy As_2S_3 was induced with the 5309- and 5682- \AA lines from a Kr^+ gas laser. The As_2Se_3 spectrum was obtained with optical excitation from a monochromator and is identical to that reported in Ref. 22. All three traces of Fig. 1 were recorded with the signal averaging capabilities of the ESR apparatus and the cold-dark backgrounds have been subtracted.

In As_2Se_3 an additional signal was observed near $g = 2.96$. This signal, which appears to be optically active, was apparent only when the background response due to Fe^{3+} was subtracted. The magnitude of the signal near $g = 2.96$ was observed to

TABLE I. Saturated densities of optically induced paramagnetic centers and the corresponding inducing photon energies for the amorphous semiconductors studied.

Glass	Inducing energy (eV)	N (centers/ cm^3)	N_s (spins/ cm^3)
As_2S_3	2.41	6×10^{16}	10^{17}
As_2Se_3	1.77	5×10^{16}	10^{17}
Se	1.98		10^{16}
As	1.08	4×10^{16}	10^{17}
GeSe_2	2.16		5×10^{15}

scale roughly with the Fe^{3+} content and may be related to some defect produced by the presence of Fe in the glass. As this response is clearly not an intrinsic property of glassy As_2Se_3 it will not be discussed further. The saturated or maximum achievable densities of optically induced ESR centers are $N_s \sim 10^{16} \text{ cm}^{-3}$ for Se and $N_s \sim 10^{17}$ for As_2S_3 and As_2Se_3 . Through the use of high-intensity laser light ($\sim \text{W}/\text{cm}^2$) whose wavelength provided a penetration depth of the order of 1 mm it was possible to excite a larger volume of the sample to the saturation density of optically induced centers than in the case of the low-intensity light from the monochromator which penetrated only 100 μm . These larger volumes of irradiated sample provided greatly improved ESR signal strengths in comparison to the previously reported results. However, although larger total numbers of spins were achieved with laser excitation, increased exposure to the high-intensity laser light in Se, As_2S_3 or As_2Se_3 (6471- \AA gas laser) failed to produce densities of ESR centers in excess of the values listed in Table I which were achieved with the 1-mW/cm² light from a monochromator. The values of N_s obtained in all other samples studied are also listed in Table I. The dashed curve in Fig. 1 represents a best-fit computer simulation of the observed ESR spectrum for Se, which will be discussed in more detail in Sec. IV and yields the principal components of the g tensor ($g_1 = 2.00, g_2 = 2.03, g_3 = 2.14$ with an error of ± 0.02). These values are identical to those reported in Ref. 22, where it was concluded on the basis of the shifts of those components relative to the free-electron g value that the observed centers are holes.

The relatively narrow resonances originally reported for As_2Se_3 and As_2S_3 (linewidths $\sim 250 \text{ G}$ and $\sim 75 \text{ G}$, respectively) in Ref. 21 are seen in Fig. 1, but in addition a second broader resonance with shoulders of width $\sim 1400 \text{ G}$ is observed which is not present in the Se spectrum of Fig. 1. The linewidths of the narrow resonances have been shown to be consistent with centers localized on the chalcogen atoms,^{21,22} while the broad shoulders have been attributed to a second center localized predominantly on an arsenic atom.^{22,23} The detailed arguments supporting these interpretations are presented in Sec. IV.

All of the optically induced effects reported for the chalcogenide glasses, including optically induced ESR, have also been observed in amorphous arsenic ($a\text{-As}$).²³ In this material the paramagnetic centers are localized on arsenic atoms, and, as expected, the optically induced ESR spectrum in $a\text{-As}$ is much broader than those observed in the chalcogenide glasses. The optically induced ESR spectrum for $a\text{-As}$ is shown in Fig. 2(a) along

with the cold-dark (pre-illumination) spectrum obtained in this material. In spite of the high purity of our samples of $a\text{-As}$ (99.999%) a cold-dark ESR signal was always observed. However, under the application of light with the appropriate wavelength (1.15 μm) the ESR signal strength was observed to increase strongly, reaching a saturated level of approximately 5 times the cold-dark intensity after prolonged illumination. Since the illuminated sample volume is apparently less than one-tenth of the total sample volume, the density of optically induced spins is at least a factor of 50 greater than the cold-dark density which presumably occurs uniformly throughout the entire sample volume. The trace in Fig. 3 represents the optically induced response obtained by subtracting the pre-illumination spectrum from the much stronger post-illumination spectrum. A comparison of this spectrum with the optically induced spectrum of Fig. 2 indicates that these two spectra are quite similar in linewidth and shape and suggests the possibility that, unlike the chalcogenides, the optical excitation may simply increase the concentration of some localized paramagnetic center that is present in the cold dark, and may not

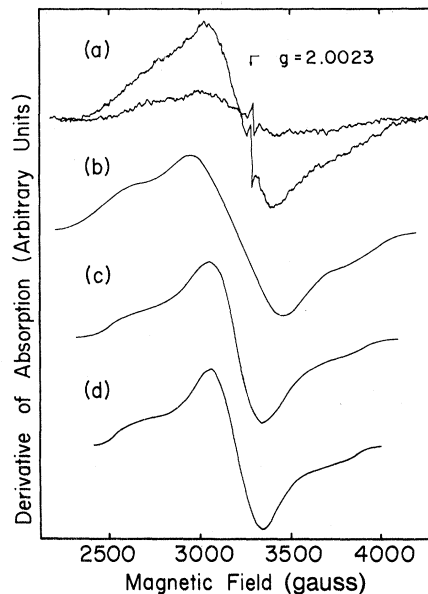


FIG. 2. (a) Optically induced ESR spectrum for $a\text{-As}$ (stronger resonance) and the cold-dark or pre-illumination spectrum obtained in this material (weaker resonance). (b) Computer simulated ESR spectrum for $a\text{-As}$ which represents the best fit to the experimental spectrum. Constraints on the wave function include localization on a single As atom. Curves (c) and (d) represent the results of allowing the best fit wave function used for (b) to be delocalized on two and three equivalent As atoms, respectively.

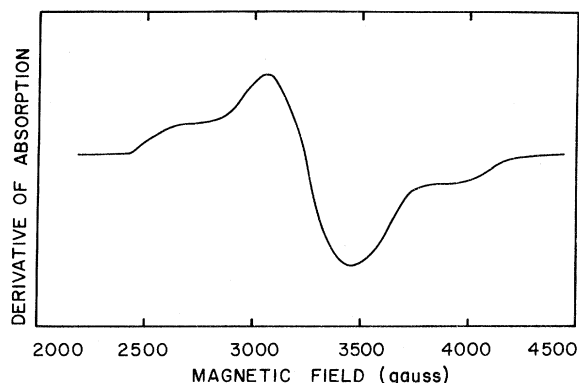


FIG. 3. Optically induced ESR spectrum obtained for α -As by subtracting the preillumination spectrum from the postillumination spectrum in Fig. 2(a).

produce a distinctly new and different center. However, there are subtle differences between the two traces, in particular the relative height of the two shoulders with respect to the central peak, which suggest that the ESR is sensitive to the difference in local bonding configuration between those sites which are optically sensitive and those which are not. From the integrated intensity of the optically induced portion of the ESR spectrum an estimated value of the concentration of optically induced paramagnetic centers of $N_s \approx 1 \times 10^{17} \text{ cm}^{-3}$ is obtained (assuming spin $\frac{1}{2}$ and $\alpha \sim 100 \text{ cm}^{-1}$ for 1.15- μm wavelength light).

The large linewidths of the α -As ESR spectra in Figs. 2 and 3, $\sim 450 \text{ G}$ for the narrower central line and $\sim 1400 \text{ G}$ for the broad shoulders, preclude any accurate measurement of the g values and indicate that the line shape is determined primarily by the large hyperfine interaction with atomic As rather than by the spin-orbit interaction. This will be discussed later in more detail.

Comparison of the As_2S_3 and As_2Se_3 glass spectra of Fig. 1 with the α -As spectrum of Fig. 2(a) indicates that the broader resonance observed in these chalcogenide glass ESR spectra (in particular, the resolved shoulders near 2600 and 3700 G) is attributable to paramagnetic centers localized on As atoms. This is demonstrated graphically in Fig. 4 where it is shown that the As_2Se_3 glass ESR spectrum can be approximated closely by a properly weighted (1:1) sum of the α -As spectrum and the glassy Se spectrum. The most important observation here is that the glassy As_2Se_3 ESR spectrum exhibits the low- and high-field shoulders near 2600 and 3700 G which characterize the α -As ESR spectrum. An inflection near 3500 G in the glassy As_2Se_3 ESR spectrum correlates well with the high-field central peak of the As center spectrum. In the As_2S_3 spectrum, the central

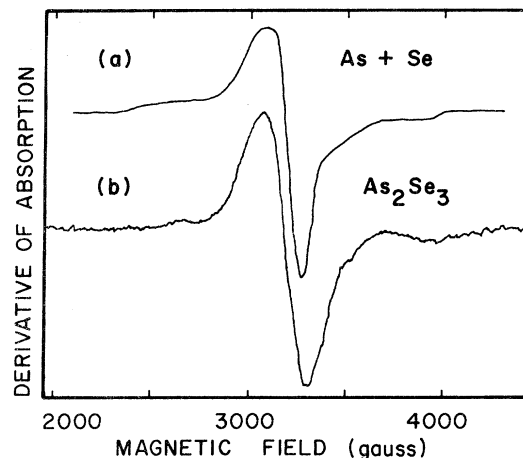


FIG. 4. Comparison of properly weighted sum (a) of optically induced ESR spectra obtained for glassy Se and α -As with the spectrum (b) obtained from As_2Se_3 glass.

peaks of the As-center spectrum near 3000 and 3400 G (see Fig. 1) are clearly resolved as shoulders on the narrower sulfur hole center resonance; the ESR signal in the As_2S_3 glass was not of sufficient strength to reveal the low-field shoulder of the As-center spectrum, but a trace run at increased gain indicated the presence of the high-field feature. Hence, both a hole center localized on the chalcogen and a center (presumably an electron) localized on the As are observed in the optically induced ESR spectra of the arsenic chalcogenides.

In order to observe the possible effects of a tetrahedrally coordinated constituent atom upon the optically induced paramagnetic states, a sample of glassy GeSe_2 was studied. This material exhibits all the photoluminescence effects (although the fatiguing effect is weak) which characterize the As chalcogenide glasses. The ESR spectrum induced in glassy GeSe_2 at $\sim 4.2 \text{ K}$ by 6328- \AA light is shown in Fig. 5. This resonance is attributed to holes most likely localized on the chalcogen (Se) but its line shape is somewhat less anisotropic than that of the centers in pure Se glass. The possible implications of this fact will be discussed later. The saturated density of the paramagnetic states estimated from the integrated ESR intensity is only $N \sim 5 \times 10^{15} \text{ cm}^{-3}$.

The growth curves of the ESR responses in α -As and As_2Se_3 with time under optical illumination are shown in Fig. 6 on a log-log scale. It is clear from this figure that the intensities of both resonances saturate at long exposure times. The dashed curves represent fits to the data assuming an exponential inducing rate $[N = N_s(1 - e^{-t/\tau_i})]$ with $\tau_i \approx 365 \text{ sec}$ in As_2Se_3 and $\tau_i \approx 11 \text{ sec}$ in α -As]. Al-

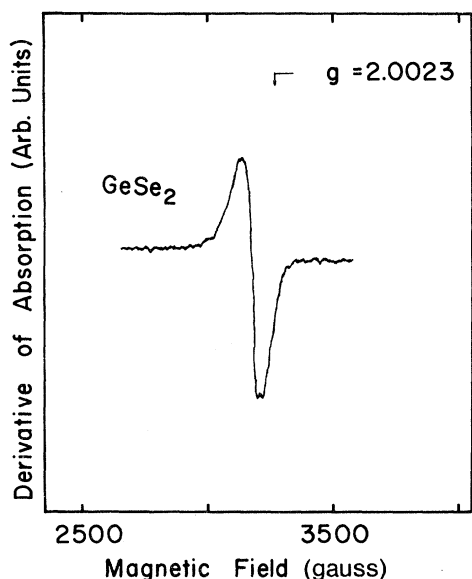


FIG. 5. Optically induced ESR spectrum in glassy GeSe_2 .

though the departures of the data from the dashed curves indicate that there exists a distribution of inducing rates in the glasses, it is apparent from Fig. 6 that the average inducing rate in *a*-As is more than an order of magnitude faster than that in As_2Se_3 . Within experimental error both the chalcogen and the As associated ESR centers in As_2Se_3 grow at the same rate. The bleaching or decay rates for *a*-As and As_2Se_3 depend upon the total inducing dose, but the decay rate for *a*-As is generally slower than that for As_2Se_3 .

Measurements of the saturation of the ESR signal in As_2Se_3 with increasing microwave power are presented in Fig. 7 for powers ranging from 0.01 to 100 mW. An analysis of this saturation behavior described in Sec. IVC yields a spin-lattice relaxation time T_1 of ~ 0.1 msec at 4.2 K.

An attempt to observe optically induced ESR spectra in amorphous Ge and Si was also carried out. Samples of amorphous Ge containing 5% hydrogen, produced by sputtering in an argon atmo-

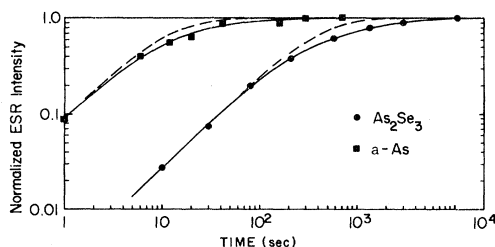


FIG. 6. Growth curves of the optically induced ESR intensities for *a*-As and glassy As_2Se_3 as a function of time under continuous optical illumination.

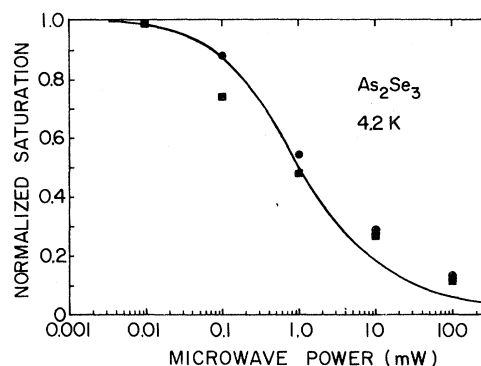


FIG. 7. Measurements of the extent of saturation of the ESR signal in glassy As_2Se_3 as a function of microwave power.

sphere contaminated with hydrogen, and pure sputtered amorphous Si were subjected to the same optical excitation procedures as were used for the chalcogenide glasses. As expected these samples exhibited the strong equilibrium or cold-dark ESR spectra which characterize the amorphous tetrahedrally coordinated semiconductors. For this reason we were faced with the problem of attempting to observe a possibly very weak effect in the presence of a strong obscuring resonance. Within these limitations, no metastable optically induced effects were observed. During the application of the exciting light the ESR intensity was reduced slightly because of the optically induced temperature rise in the sample, but the signal strength returned to normal when the light was removed. On the basis of these measurements carried out near 4.2 K it can only be said that fewer than 10^{17} - cm^{-3} spins were optically induced in the amorphous Ge sample while the limit for the sputtered Si film was 10^{18} cm^{-3} . It is entirely possible that some optically induced effects may yet be observed in films in which the background ESR intensity due mainly to unpaired spins associated with voids is greatly reduced by annealing or hydrogen doping.

B. ESR intensity determinations

The saturated densities of induced paramagnetic spins, N_s (see Table I), were determined at 4.2 K by comparison of the observed ESR intensities (second integrals of the ESR derivative spectra) with a calibrated line-standard sample containing 10^{13} spins/ cm^3 .

In the absence of saturation of the spin system by the microwave field, the experimental ESR signal is proportional to the modulation field H_m , the microwave field H_i , and the spectrometer gain G . In practice, all three of these normalization quantities differed by at least an order of magnitude between the sample and the standard be-

cause the optically induced ESR lines are broad and weak in comparison to the resonance in the calibrated sample. Corrections for H_m , H_i , and G are estimated to introduce errors by a factor of ~ 2 in the calculated values of N_s . In addition, as will be described below in Sec. IV C, the optically induced ESR spectra are partially saturated even at the lowest attainable microwave power (0.01 mW) at 4.2 K. This fact implies that the direct proportionality between the ESR signal and the microwave field is only approximately correct. The final significant error in the calculation of N_s concerns an estimate of the active sample volume which is controlled by the penetration depth of the inducing light ($\sim 10^{-2}$ cm). Uncertainties in this estimate also introduce errors on the order of a factor of 2. Given these uncertainties, the absolute values of N_s quoted in Table I are known only within about an order of magnitude; however, the relative magnitudes of N_s among different entries of the table are accurate within about a factor of 3. Because of the small active sample volume ($\sim 5 \times 10^{-3}$ cm³), the total number of optically induced spins actually observed is between $\sim 10^{13}$ and $\sim 10^{14}$, which explains the small signal-to-noise ratio in the experimental ESR traces.

C. Optically induced below-gap absorption

In glassy As_2Se_3 , $\text{As}_2\text{Se}_{1.5}\text{Te}_{1.5}$, and amorphous As, 5- or 10-min irradiations with the band-edge photon energies given in Table I produced 10% to 15% reductions of sample transmission in the band-edge to mid-gap spectral range. Such reductions in optical transmission correspond to an induced absorption coefficient $\alpha > 10$ cm⁻¹ in the approximately 100 μm thick penetration depth of the exciting or inducing light. The optically induced absorption spectra for As_2Se_3 , As_2S_3 , and α -As are shown in Fig. 8 along with their respective cold-dark or preillumination band-edge absorption curves. While the As_2Se_3 and α -As spectra were induced by the 1-mW/cm² light from a tungsten source and monochromator, the 5145-Å light from a defocused argon-ion laser (~ 500 mW/cm²) was used to induce the mid-gap absorption in As_2S_3 glass. This was done because the intensity available at blue green wavelengths from the tungsten source was insufficient. Several minutes of exposure to the 1-mW/cm² light were required to bring the induced absorption to its saturated level in As_2Se_3 and α -As, while several seconds of exposure to the laser light were sufficient for As_2S_3 .

If it is assumed that the upper limit for the optical cross section of an optically induced center is given by the cross section of an isolated defect such as an F center with unity oscillator strength,²⁴

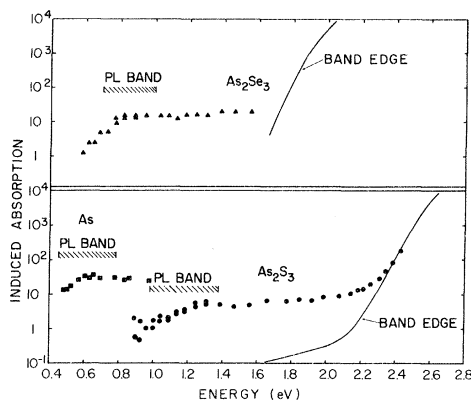


FIG. 8. Optically induced absorption spectra for glassy As_2Se_3 , As_2S_3 , and As. Preillumination band-edge absorption curves are given for As_2Se_3 and As_2S_3 but such low-temperature data are not available for α -As.

then it is possible to obtain estimated lower limits for the total density of induced states, N , from the induced absorption coefficient in each material. The values of N estimated in this way from the absorption data are listed in Table I for the various glasses. Note that in all cases where comparisons are made these estimates are in substantial agreement with the values of N_s obtained from the ESR intensities.

In all materials studied the spectral extent of the induced optical absorption ranges from the vicinity of the low-energy limit of the photoluminescence band in the glass up to the onset of strong interband absorption. Bleaching experiments carried out in As_2Se_3 , $\text{As}_2\text{Se}_{1.5}\text{Te}_{1.5}$, and α -As demonstrated that irradiation of the sample (after the absorption had been induced by band-gap

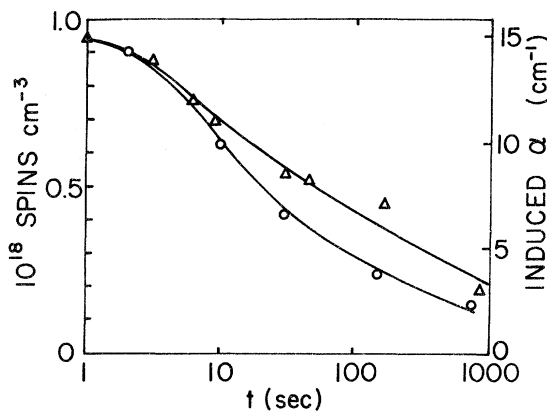


FIG. 9. Reduction in optically induced absorption coefficient (triangles) and induced ESR intensity in glassy As_2Se_3 as a function of continuous exposure to 3 mW/cm² of 1.24-eV (bleaching) light.

light) with near-ir light at any wavelength within the induced absorption band would "bleach" or reduce the strength of the induced absorption as well as the induced ESR intensity. This bleaching effect is illustrated in Fig. 9 which shows the reduction in induced α and induced ESR intensity in glassy As_2Se_3 under continuous exposure to 3 mW/cm² of 1.24-eV light, which falls near the center of the induced absorption band for this material. Since the mechanism for bleaching depends upon the induced absorption itself, as the absorption is bleached or reduced, the bleaching process naturally becomes progressively less efficient. The similarity of the bleaching (and growth) rates for both the ESR and the optical absorption confirms that these two effects are due to the same centers within the forbidden energy gap.

D. Crystalline As_2S_3 and As_2Se_3

Attempts were made to observe the optically induced ESR in synthetic crystals of As_2Se_3 and natural crystals of As_2S_3 (orpiment). The experimental conditions were identical to those which were used in the successful experiments on the glasses. The synthetic As_2Se_3 crystals (which were doped with Tl during growth) were quite pure with respect to paramagnetic impurities and no significant cold-dark ESR was observed in the vicinity of $g=2$. Irradiation under conditions which produced $\sim 10^{17}$ spins/cm³ in glassy As_2Se_3 failed to produce an observable ESR in the crystalline As_2Se_3 . This enables us to place a conservative upper limit of $\leq 10^{16}$ optically induced spins/cm³ which could be present in the crystal and not be detected by our experiment. The natural crystals of orpiment also exhibited no optically induced ESR signal under conditions which produced $\sim 10^{17}$ spin/cm³ in glassy As_2S_3 . In this case, paramagnetic impurities in the mineral produced a cold-dark resonance in the vicinity of $g=2$ which places the observability limit for an optically induced ESR at $\leq 5 \times 10^{16}$ spins/cm³.

Within the limits of the accuracy of these measurements, it can be said that in the arsenic chalcogenides the optically induced localized paramagnetic states are apparently unique to the disordered phase.

IV. ANALYSIS OF THE ESR SPECTRA

The spin Hamiltonian which describes the optically induced ESR spectra observed in this study contains both the electronic Zeeman and hyperfine terms:

$$H = \beta \vec{H} \cdot \vec{g} \cdot \vec{S} + \vec{S} \cdot \vec{A} \cdot \vec{I}, \quad (1)$$

where \vec{g} is the electronic spin gyromagnetic ten-

sor, \vec{A} the hyperfine tensor, \vec{H} the applied magnetic field, and \vec{S} and \vec{I} are, respectively, the electronic and nuclear spin vectors. The first term can be diagonalized analytically to determine the energy levels of the system while the second term must be evaluated using perturbation theory. If it is assumed that $S = \frac{1}{2}$ and that the principal axes of \vec{g} and \vec{A} are coincident, then the resonance condition is given by

$$h\nu = g \mu_B H + Am, \quad (2)$$

where

$$\begin{aligned} g^2 &= g_a^2 \sin^2 \theta + g_s^2 \cos^2 \theta, \\ g_a^2 &= g_1^2 \sin^2 \phi + g_2^2 \cos^2 \phi, \\ g^2 A^2 &= g_a^2 B^2 \sin^2 \theta + g_s^2 A_3^2 \cos^2 \theta, \\ g_a^2 B^2 &= g_1^2 A_1^2 \sin^2 \phi + g_2^2 A_2^2 \cos^2 \phi. \end{aligned}$$

In Eq. (2), θ and ϕ are Euler angles of rotation, and the hyperfine terms have been calculated to first order in perturbation theory.²⁵ The quantities A_i , g_i are the principal components of \vec{A} and \vec{g} , respectively, and m is the magnetic quantum number of the nuclei with which the electronic spin is interacting via the hyperfine term.

The resonance field H in Eq. (2) depends on the orientation of the paramagnetic site with respect to the field through the variables θ and ϕ . In a polycrystalline sample, the paramagnetic sites are randomly oriented, and the observed spectrum is an average over all possible orientations. Such an average is called a powder pattern. In a glassy or amorphous solid one must often perform an additional average over the random variations in local environments surrounding the paramagnetic spin. This average, which is necessitated by the structural disorder inherent in the amorphous state, must be evaluated numerically with an assumed model for the paramagnetic center. Because of the lack of structure in the optically induced ESR lines and because of limited knowledge of the specific paramagnetic centers, detailed averages over local environments will not be attempted here. In principle, an additional term should be added to Eq. (1) to account for dipolar interactions between paramagnetic electrons, but in practice this contribution to the Hamiltonian is approximated by a convolution of the delta function resonance condition [Eq. (2)] with a Gaussian function whose width σ characterizes the unresolved dipolar interactions. The Gaussian-broadened powder pattern, with or without an additional average over local environmental variations, is usually presented as a derivative spectrum to facilitate comparisons with experimental traces. Details concerning the evaluation

TABLE II. Principal components of the g tensors and the widths of the unresolved dipolar interactions for the optically induced ESR spectra in various amorphous semiconductors.

Glass	g_1^a	g_2^a	g_3^a	σ (gauss)
As ₂ S ₃	2.00	2.02	2.07	40
As ₂ Se ₃	2.00	2.03	2.14	50 ^b
Se	2.00	2.03	2.14	50
As	2.0	2.0	2.0	130
GeSe ₂	2.00	2.01	2.09	50

^aAll g values are ± 0.02 except those for As which are ± 0.2 .

^bEstimated from Se data.

of ESR spectral parameters from polycrystalline or glassy solids are available elsewhere.²⁵

A. Chalcogen hole center

In Se only the Zeeman (first) term of Eq. (1) is necessary to describe the observed ESR spectrum of Fig. 1(c) because most Se atoms have zero nuclear spin. A computer simulation of the first derivative spectrum is indicated by the dashed line in Fig. 1(c). This simulation was performed as described above with the parameters indicated in Table II. The asymmetry and the relative heights of the maximum positive and negative excursions of the derivative trace were compared with a set of computer simulated traces employing different spin-Hamiltonian parameters to determine the errors quoted in Table II. In a similar fashion the narrow line observed in glassy As₂Se₃ is best fit within experimental error with parameters identical to those employed for Se. Principal g values for the narrow line in As₂S₃ are also shown in Table II.

As will be discussed below, ⁷⁵As has spin $I = \frac{3}{2}$ and large values of the atomic hyperfine coupling constants. One thus expects a large hyperfine

broadening of any ESR center which is predominantly localized on an As atom. We conclude therefore that the narrow resonances in As₂Se₃ and As₂S₃ are localized almost exclusively on the chalcogen atoms.

In what follows we assume that the narrow lines observed in Se, As₂Se₃, and As₂S₃ result from centers which are localized predominantly on a single atom, and we examine the consequences of this assumption at the end of the discussion. If localized, these centers are most likely holes since all the g values (Table II) are greater than or equal to the free-electron value of $g_e = 2.002$. The three principal g values, g_i , are determined by the admixture of excited states into the ground state via the spin-orbit interaction according to the well known relation²⁶

$$g_i = g_e + 2\lambda \sum_{n \neq 0} \frac{\langle 0 | L_i | n \rangle \langle n | L_i | 0 \rangle}{E_0 - E_n}, \quad (3)$$

where the sum is over excited valence-band states; λ is the spin-orbit coupling constant (for the appropriate chalcogen), L_i are the orbital angular momentum operators, and the sum depends on details of the bonding configurations in the valence band.

A variety of amorphous materials containing the chalcogen elements, O, S, Se, and Te display remarkably similar valence-band densities of states.²⁷⁻³⁰ In particular the highest-lying level is in all cases a chalcogen lone pair p band, and there is essentially no s - p hybridization of any of the chalcogen p levels. In addition the widths of the valence bands are nearly identical in As₂S₃, As₂Se₃, Se, and As₂Te₃ and about a factor of two greater in SiO₂ (see Table III). It is apparent from Eq. (3) that for paramagnetic holes on different atoms whose bonding configurations are equivalent, the departures of the principal g values from the free-electron value $\Delta g_i = g_i - g_e$ should scale with λ for the atom on which the cen-

TABLE III. Departures (Δg_i) of the principal components of the g tensor from the free-electron value and the spin-orbit coupling constant for ESR spectra in some chalcogenide and oxide glasses. Also given are p -like valence-band widths determined from photoemission data.

Material	Δg_3	$\lambda(\text{cm}^{-1})^a$	Valence band-width (eV) p levels only	$\frac{\Delta g_3}{\lambda}$ (arbitrary units)
Se	0.14	1688	5 ^c	1
As ₂ Se ₃	0.14	1688	5 ^c	1
As ₂ S ₃	0.07	382	5 ^c	2
SiO ₂	0.02	151	9 ^d	2
B ₂ O ₃ ^b	0.02-0.05	151	...	2-4

^aValues for neutral (VLA) atom.

^bAverage of several borate glasses.

^cReference 30.

^dReferences 27 and 29.

ter is localized. Since the upper chalcogen valence-band levels are entirely p -like and of similar shapes and widths in oxides, sulfides, selenides, and tellurides (within a factor of two) one expects Δg_i to scale with λ within factors of two for values of λ which vary by a factor of 10 over these elements (see Table III).

Paramagnetic centers attributed to holes localized on oxygen p orbitals have been exhaustively studied in several oxide crystals and glasses.³¹ These centers characteristically have one component of the g tensor very near the free-electron value and two components with positive values of Δg_i . In glassy SiO_2 and silicate glasses a hole center is observed³² after x or γ irradiation. The values of Δg_i for this center agree well with those observed in the semiconducting chalcogenides when scaled by the appropriate values³³ of λ as indicated in Table III. In glassy B_2O_3 and borate glasses a similar hole center is observed (a boron-oxygen hole center)³¹ whose values of Δg_i again scale well with λ . In Table III we have chosen to compare the value of Δg_3 for the oxides, selenides, and sulfides because this component has the largest magnitude and is the most accurately determined component in the sulfide and selenide spectra. The ratios of $\Delta g_3/\lambda$ as shown in the final column of this table are in fact constant within factors of two for most materials.

It is interesting to note that an extension of these arguments to $\text{As}_x\text{Te}_{1-x}$ glasses³⁴ would predict a value of $\Delta g_3 \approx 0.4$ and therefore a width for the hole center line essentially indistinguishable from that observed in the central portion of the α -As line [Fig. (2)]. In glassy AsTe a spectrum is observed which is very similar to (but nonetheless distinguishable from) that found in α -As; the latter could be the superposition of an isotropic hole center resonance which is broader than that associated with Se and the resonance from the center associated with As.

Detailed arguments^{31, 35} suggest that the oxide centers are localized either on dangling bond oxygen p orbitals or on nonbonding oxygen p orbitals, although it is impossible to distinguish unambiguously between these two cases from knowledge of the g tensor alone. When the oxygen atom is bonded to atoms with nonzero nuclear spin such as ^{11}B , ^{10}B , ^{29}Si and others, a small resolved hyperfine interaction is observed. In these cases one can sometimes distinguish between a hole on a nonbonding oxygen p orbital and a hole on a dangling bond oxygen p orbital depending on whether the hyperfine interaction is with one or two neighboring nuclei. The magnitude of the isotropic part of this resolved hyperfine interaction is such that $\approx 1\%$ of the unpaired spin is localized in an S

wave function on the neighboring atom or atoms. A similar, but unresolved, hyperfine interaction with ^{75}As may be responsible for the subtle differences near $g = 2.00$ between the experimental As_2Se_3 spectrum and the sum of the Se and As experimental spectra of Fig. 4. However, since no resolved hyperfine structure has yet been observed in the optically induced centers, it is impossible to distinguish between a nonbonding orbital and a dangling bond.

Although the general scaling relationships of the g values with λ for oxides, sulfides, and selenides provide convincing evidence for the identification of the optically induced chalcogen ESR centers with a hole localized on a nonbonding chalcogen p orbital, for several reasons more detailed comparisons must be attempted only with great caution. For example, the resolution of the photoemission data is presently only sufficient to provide the general features of the valence band. In addition, the ionic character of the bonding changes significantly from the oxides to the other chalcogenides. While the Si-O and B-O bonds contain nearly equal ionic and covalent contributions, the As-S and As-Se bonds are estimated to be more than 90% covalent. Finally, the optically induced ESR spectra themselves at present provide detail insufficient to determine more than the most basic properties of the centers.

We conclude this analysis of the chalcogen hole centers in Se, As_2Se_3 , and As_2S_3 with some speculation concerning the lack of resolved structure in these ESR responses. In the radiation-damaged oxide glasses resolved structure is observed in both the g and hyperfine tensors even though the values of Δg_i are much smaller than in the semiconducting glasses. The lack of resolution in the latter glasses is not due to unresolved dipolar interactions because these are the same order of magnitude as in most oxide glasses. Two additional possibilities exist which could explain this lack of resolution: (i) a greater distribution in site-to-site bonding configurations for the optically induced centers in the semiconducting glasses than for the radiation-damage centers in the oxide glasses, or (ii) delocalization of the optically induced centers over more than one chalcogen atom.

The available data are insufficient to provide a distinction between these two possibilities; however two positive comments can be made. First, preliminary ESR experiments on semiconducting glasses electron irradiated at 77 K indicate that the radiation-induced centers are characteristically *different* from the optically induced centers.³⁶ The electron-irradiated samples in general display similar ESR spectra but with increased resolution,

as in the oxides, and without optical sensitivity. Second, the similarities in the g tensors and the lack of large hyperfine effects in both classes of ESR spectra suggest that the optically induced centers are not *highly* delocalized. With extensive delocalization the g values would begin to take on the properties of the valence band rather than the localized bond, and similarities with the oxides would become fortuitous. We thus conclude that the wave functions of the hole centers in Se, As_2Se_3 , and As_2S_3 consist primarily of nonbonding or dangling bond chalcogen p orbitals, but the precise extent of localization remains a highly significant question.

B. Arsenic center

Unlike the chalcogen hole centers just described, the localization of the optically induced ESR centers observed in α -As can be well defined. Because of the large hyperfine interaction for a spin localized predominantly on an ^{75}As atom, the second terms of Eqs. (1) and (2) dominate the shape of the ESR response in α -As. The g tensor is found to be isotropic and identical in magnitude with the free-electron value within the error quoted in Table I. The dominance of the hyperfine term was confirmed for the cold-dark resonance in α -As by measurements at 35 GHz (Ka band). The widths of the central peak at 35 and 9 GHz are identical as expected since the hyperfine term of Eq. (2) is independent of magnetic field.

It will be shown below that the salient features of the α -As optically induced ESR spectrum (i.e., the central peak and resolved shoulders of Fig. 2) are inconsistent with the assumption that the paramagnetic spin is delocalized over more than a few As atoms. For simplicity we first assume that the center is localized predominantly at a single As site and discuss the detailed possibilities. Then we will examine the consequences of allowing the unpaired spin to become more and more delocalized on equivalent As atoms.

For the case of localization on a single As atom the most general form of the s - p hybridized wave function which contributes to the hyperfine interaction in a powdered sample is given by

$$\Psi = c_s |s\rangle + c_{p_x} |p_x\rangle + c_{p_y} |p_y\rangle. \quad (4)$$

Use of the hyperfine interaction alone to determine the wave function involves one possible ambiguity. Equal densities of all three orthogonal p functions can be added arbitrarily to Ψ because isotropic admixtures of all three p states do not contribute to the hyperfine term.³⁷⁻³⁹ For this reason only two p orbitals need to be considered in Eq. (4) and the normalization condition must be written as

$c_s^2 + c_{p_x}^2 + c_{p_y}^2 \leq 1$ even though the spin is localized at a single As site. Fortunately, this ambiguity will turn out to be unimportant for the case of α -As. The wave function Ψ yields the following values for the hyperfine coupling constants which enter into Eq. (2):

$$\begin{aligned} A_1 &= A_0 c_s^2 + B_0 (2c_{p_x}^2 - c_{p_y}^2), \\ A_2 &= A_0 c_s^2 + B_0 (2c_{p_y}^2 - c_{p_x}^2), \\ A_3 &= A_0 c_s^2 + B_0 (c_{p_x}^2 + c_{p_y}^2), \end{aligned} \quad (5)$$

where A_0 and B_0 are the respective atomic s and p hyperfine coupling constants for As. Values of A_0 and B_0 for As have been calculated by several authors.³⁷⁻³⁹ In what follows we use values due to Hurd and Coodin³⁷ ($A_0 = 4500$ G, $B_0 = 119$ G) which appear to be the most accurate; values approximately 25% smaller than these have also been suggested. Although A_0 and B_0 are known only within an error of about $\pm 30\%$, the ratio A_0/B_0 , which determines the anisotropy of the observed ESR spectrum through Eqs. (5) and (2), is known with much greater precision ($\pm 2\%$). Note that only the magnitudes of A_1, A_2, A_3 can be determined from the ESR spectrum since these quantities enter only as squares in Eq. (2).

From the magnitudes of A_0 and B_0 for As it is apparent that the unpaired spin is not entirely localized in either s or p wave functions because the widths of the predicted ESR responses [obtained using Eqs. (5) and (2) to calculate the powder pattern] in these two cases are greater than 10 000 G and less than 720 G, respectively. The actual width of the shoulders in the experimental trace of Fig. 2 is ~ 1400 G and is inconsistent with both of these predictions.

The next simplest approximation, the admixture of a single p state to the s state, is capable of providing good agreement with experiment. In this case, Eq. (5) becomes axially symmetric and reduces to the form

$$\begin{aligned} A_{\parallel} &= A_0 c_s^2 + 2B_0 c_p^2, \\ A_{\perp} &= A_0 c_s^2 - B_0 c_p^2. \end{aligned} \quad (6)$$

The best fit to the experimental spectrum within the constraints of the above equations is shown in Fig. 2 (curve b) and occurs for $A_{\parallel} = 400$ G and $A_{\perp} = 57$ G or $c_s^2 = 4\%$, and $c_p^2 = 96\%$. The admixture of a second p function using Eq. (5) deteriorates the fit by broadening the central derivative peak or by lowering the intensity of the central peak with respect to the shoulders. Similarly, any attempt to add in an isotropic mixture of $p_x, p_y,$ and p_z also deteriorates the fit because the s density must then be reduced ($c_s^2 + c_p^2 \leq 1$). The fit to the experimental spectrum is extremely sensitive to the amount of

assumed s density because the positions of the shoulders are strongly dependent on the value of c_s^2 . Deviations in c_s^2 of only $\pm 1\%$ produce a discernible deterioration of the fit. For this reason, the main uncertainty in the value of c_s^2 results from uncertainties in the estimates of A and B . Thus, within the assumption of localization on a single As atom, the experimental ESR spectrum is best fit when the unpaired spin exists predominantly in a single p orbital with a small ($\sim 5\%$) s admixture.

We next examine the consequences of allowing the unpaired spin to be delocalized on more than one equivalent As atom. The interaction of the unpaired spin S with N equivalent nuclei of spin I can be treated formally as an interaction of the spin with a fictitious nucleus of spin NI . The qualitative result of allowing the spin to become more and more delocalized is to deteriorate progressively the definition and the magnitude of the shoulders with respect to the central portion of the derivative spectrum. A specific illustration of these effects is shown in Fig. 2 where curves c and d represent the results of allowing the best-fit wave function of the unpaired spin as determined above to be delocalized on two and three equivalent As atoms, respectively. The effective spin-Hamiltonian parameters for these cases are listed in Table IV. The effective linewidths σ_{eff} used for the three calculations were varied roughly in proportion to the ratios of unresolved dipolar interactions with As nearest neighbors for $\text{As}_{(1)}$, $\text{As}_{(2)}$, and $\text{As}_{(3)}$ clusters, respectively. This procedure constituted an attempt to retain roughly the same resolution for all three spectra. Note that in curve d the relative height of the shoulders is reduced with respect to the central peak. The comparison of curve d with the experimental trace (curve a) is certainly not as good as the comparison of the spin localized on a single atom with experiment (curves b and a). The uncertainties in the experimental data and in the calculations are sufficient that one cannot rule out the possibility that a substantial proportion of the optically induced ESR centers in α -As is delocalized over three As atoms. However, the fit with experiment

rapidly deteriorates as the number of atoms is increased beyond three, and the possibility that a substantial number of the ESR centers is localized on more than three atoms can be excluded.

The cold-dark response [Fig. 2(a)] displays subtle differences in the wings from the optically induced line from which the cold-dark resonance has been subtracted (Fig. 3). Note that the relative heights of the shoulder with respect to the central peak are less in the optically induced trace of Fig. 3. This fact indicates that there are probably subtle differences between the paramagnetic centers present in the cold dark in α -As and those which are optically induced. The decrease in intensity of the shoulders in the optically induced spectrum is consistent with the speculation that these centers are slightly less localized than the dangling bonds present in the cold dark.

As in the case of the chalcogen hole centers, the Gaussian broadening which is necessary to fit the experimental spectrum is about an order of magnitude greater than that which would be expected from dipolar effects alone. This fact suggests that, because of random distortions in the local environments, not all As sites are identical and that the localization of the unpaired electrons varies somewhat from site to site within the constraint that most of the centers are localized on less than about three As atoms.

C. Spin-lattice relaxation times

In As_2Se_3 the optically induced ESR signal at 4.2 K was sufficient to study the dependence of the ESR intensity in microwave power. The ESR signal depends sublinearly on the microwave field H_1 even at the lowest obtainable microwave powers ($P \geq 0.01$ mW), although the signal does approach an unsaturated condition at 0.01-mW power. The line shape does not change shape on saturation and there is no evidence for a turn over in the ESR intensity as a function of H_1 at high microwave fields. These two facts indicate the applicability of the model developed by Portis⁴⁰ and refined by Hyde⁴¹ for the saturation behavior of an inhomogeneously broadened ESR line in the absence of spin diffusion. In this model the saturation of the imaginary part of the microwave susceptibility

$$\chi''(\omega) = \frac{1}{2} \chi_0 h(\omega - \omega_0) \frac{\pi}{(1 + \gamma^2 H_1^2 T_1^2)^{1/2}}, \quad (7)$$

where χ_0 is the temperature-dependent dc susceptibility, $h(\omega - \omega_0)$ is the normalized distribution in local resonance fields, γ is the gyromagnetic ratio, and T_1 is the spin lattice relaxation time.⁴²

Figure 7 is a plot of the normalized saturation factor $(1 + \gamma^2 H_1^2 T_1^2)^{1/2}$ for the chalcogen and arsenic

TABLE IV. Spin Hamiltonian parameters for α -As optically induced ESR center (simulation includes quadrupolar terms).

Center	A_{\parallel} (gauss) ^a	A_{\perp} (gauss) ^a	σ_{eff} (gauss)
$\text{As}_{(1)}$	400	57	150
$\text{As}_{(2)}$	200	28	100
$\text{As}_{(3)}$	133	19	70

^aAll values ± 50 G.

centers in As_2Se_3 at 4.2 K. The solid curve is a best fit to the data using Eq. (7) and yields an estimate of the order of magnitude of T_1 of ~ 0.1 msec. The two centers in As_2Se_3 both saturate at the same rate within experimental error. Although no detailed data were taken for α -As, the optically induced ESR centers in the material are estimated to exhibit a value of T_1 approximately a factor of three shorter than the centers in As_2Se_3 . As is observed for nuclear spin-lattice relaxation in glasses, these values of T_1 are at least an order of magnitude faster than values commonly encountered in crystalline materials at the same spin densities.⁴⁰ The origin of the increased relaxation rates lies almost certainly in the anomalous low-frequency vibrational properties of glasses such as those invoked to explain the increased nuclear spin-lattice relaxation rates in glasses.

V. DISCUSSION

All of the evidence currently available points to the conclusion that the optically induced, metastable, paramagnetic centers are an intrinsic feature of semiconducting glasses. The analysis of the ESR spin-Hamiltonian parameters described previously suggests that the paramagnetic centers are localized on major constituent atoms and not on impurities. Also, the saturated densities of spins N_s do not appear to depend on impurity content but do depend on the local structural order and the coordination number of the major constituent atoms. Furthermore, the optically induced centers are characteristically different from the usual paramagnetic defects produced in glasses by x-ray, γ -ray, or electron irradiation. We have demonstrated this by electron irradiating chalcogenide glasses at 77 K and studying the resultant ESR spectra.³⁶ (This work will be published in detail elsewhere but the basic results of these studies are pertinent to the present discussion.) The electron irradiation produced an ESR spectrum with better resolved spectral features than the optically (band-edge light) induced ESR spectra, although the asymmetries in the line shape are similar. This implies that the radiation-induced defects are less distorted or more highly localized than the optically induced centers. The electron-irradiated spectrum could not be optically bleached, and illumination with Urbach tail light produced the usual optically induced spectrum superimposed on this spectrum, indicating that two fundamentally different centers are involved.

The detailed analysis of the ESR spectra presented in Sec. IV indicated that if the center associated with the chalcogen is localized, then it is

a hole center localized predominantly in a chalcogen nonbonding p orbital. In the arsenic chalcogenides the localization at the As center can be established from the ESR line shape, but it can only be *assumed* that this center is the conjugate of the chalcogen hole center and therefore that the center localized on an As p orbital is an electron center. We wish to emphasize that while charged centers, dangling bonds, homo (wrong) bonds or valence alternation⁴³ are all reasonable candidates for the native structural anomalies or defects which give rise to the optically induced paramagnetic centers, our results do not provide a unique identification of these structural anomalies or defects. The implications of this statement are discussed in more detail at the conclusion of this section where the relationships of the ESR data to the predictions of several proposed models are discussed.

In any consideration of possible mechanisms for the generation of the optically induced paramagnetic states one must simultaneously consider the other optically induced effects which are observed to occur under similar optical excitation conditions. These effects, which include photoluminescence (PL)¹⁰⁻¹² and photodarkening or photostructural processes,⁴⁴⁻⁴⁷ exhibit several features which correlate with the behavior of the induced paramagnetism and optical absorption in the chalcogenide glasses.

Several experimental facts have led us to conclude that the optically induced absorption and paramagnetism in amorphous semiconductors are closely associated with the PL process which occurs in these materials. All three effects are characterized by the same excitation photon energies ($\alpha \cong 100 \text{ cm}^{-1}$); during continuous excitation at these energies both the optically induced absorption and ESR intensity grow²¹⁻²³ while the PL efficiency decreases or "fatigues"^{10,11,48}; subsequent irradiation with mid-gap light bleaches (reduces) the induced absorption and the ESR intensity and restores the "fatigued" PL efficiency. These facts are consistent with the suggestion that the diamagnetic radiative recombination centers which become inactive during progressive fatigue of PL are associated with the production of the growing ESR intensity and mid-gap absorption. In addition, for those glasses in which most of the initial luminescence intensity can be fatigued (i.e., Se and the As-containing chalcogenide glasses), the measured saturated densities N_s of the optically induced centers listed in Table I are roughly equivalent to the densities of radiative recombination centers as estimated from the PL excitation spectra.¹⁰ In GeSe_2 the initial efficiency of the luminescence is comparable to that observed in the As-containing chalcogenides but the fatigued-

ing process is much less effective.^{49,50} This fact is consistent with the low values of N_s listed in Table I for GeSe₂.

Some features of the photostructural or photo-darkening processes may also be associated with the optically induced absorption and paramagnetism in amorphous semiconductors, but the detailed correspondences are not as well determined as in the case of the PL results. It is well known that irradiation of chalcogenide glasses with band-gap light can cause shifts of the fundamental absorption edge to lower photon energies which are often accompanied by changes in the x-ray diffraction spectra for the glasses.⁴⁵⁻⁴⁷ There are at least three types of band-edge shift which depend on the sample preparation conditions and the intensity of band-gap light which is employed. Some photostructural changes are irreversible, some are reversible only thermally, and some are reversible both optically and thermally. Since those effects which are reversible only thermally have been observed to produce measurable changes in the x-ray diffraction spectrum, of the order of at least 10^{20} cm⁻³ local bonding changes must be involved. This number is much greater than the typical saturated densities of paramagnetic spins ($\sim 10^{17}$ cm⁻³) induced in these materials. It is tempting to speculate that only the optically reversible portion of the photostructural changes is directly related to the induced paramagnetism and that this number is on the order of 10^{17} and not 10^{20} cm⁻³. However, given the incomplete nature of the data, one cannot rule out the possibility that while some 10^{20} cm⁻³ optically induced bonding changes can be produced, only those changes which are associated with or occur in the vicinity of some inherent defect or anomaly in the equilibrium glass structure can result in the formation of a *metastable* paramagnetic center. It is then the density of these structural anomalies that limits the attainable density of the paramagnetic centers.

Fritzsche, Ovshinsky, and others⁵¹⁻⁵³ have pointed out that the apparent changes in local bonding configuration responsible for the various photostructural effects are favored in materials having low covalent coordination numbers and containing group VI elements with nonbonding (lone-pair) *p* orbitals. Band-gap light can excite a nonbonding electron from its valence-band lone-pair state to an antibonding conduction-band state. The subsequent structural distortion and availability of the remaining unpaired lone-pair electron for bonding could result in a local bonding rearrangement. Such local bonding rearrangements could explain the shifts in the band edge and the changes in the x-ray spectra as well as the formation of metastable paramagnetic states. This

explanation is applicable only to glasses containing chalcogens (including oxygen) and would imply that these effects cannot occur in amorphous Ge and Si. The failure to observe optically induced ESR in amorphous Ge and Si films is consistent with this explanation as are the facts that PL does not occur in pure films of amorphous Si, only in hydrogen doped,⁵⁴ and the PL in hydrogen-doped amorphous Si does not exhibit the fatiguing effect.

Further information concerning the structural anomalies or defects which are associated with the induced optical absorption and paramagnetism in amorphous semiconductors can be deduced through an analysis of the compositional dependence of the induced ESR. For example, differences in the number of optically induced ESR centers in GeSe₂ ($\sim 5 \times 10^{15}$ cm⁻³) relative to those in the arsenic chalcogenides ($\sim 10^{17}$ cm⁻³) may be related to the differences in atomic coordination number for As and Ge.⁵⁵ The two-dimensional structural basis provided by the three-coordinated As atoms in As-chalcogenide glasses contrasts strongly with the three-dimensional character produced by the introduction of tetrahedrally coordinated Ge atoms. Three-dimensionally cross-linked structural networks in glasses such as GeSe₂ are expected to be "stiffer" and far less photosensitive⁵² than the As-chalcogenide glasses. Furthermore, the extensive *s-p* hybridization which occurs in the four bonding Ge valence-band orbitals contrasts sharply with the solely *p* character of the highest-lying As and chalcogen valence-band orbitals. Such factors might well be responsible for the reduced photosensitivity of glassy GeSe₂ for photodarkening or photostructural effects and for the formation of the optically induced metastable paramagnetic states. However, this reasoning does not explain the reduced photosensitivity for the formation of metastable ESR states in Se. The optically induced ESR spectrum in glassy GeSe₂, (Fig. 5) which is also attributed to holes, differs from the pure Se and As₂Se₃ spectra in the values of the deviations of the principal components of the *g* tensor from the free-electron *g* value. These differences are a clear indication of the sensitivity of the optically induced ESR as a probe of changes in local structural order with glass composition. The asymmetry of the line and its linewidth indicate that this optically induced hole center is probably localized on a Se atom as in the case of the arsenic chalcogenides. However, the *g*-value differences are probably manifestations of subtle differences in the bonding configuration (valence-band energy levels) for the hole in GeSe₂ relative to the configuration characteristic of glassy Se and As₂Se₃. Of course, the possibility of substantial overlap

with a Ge atom cannot be completely ruled out.

Several different models have been proposed to explain the localized states in the gap of amorphous semiconductors. Some of the models, such as those of Mott and co-workers,¹⁹ Street and Mott,¹⁸ or Kastner *et al.*⁴³ invoke very specific types of structural defects. Others (Anderson,¹⁷ Economou *et al.*,²⁰ Emin⁵⁶) provide a general description of the existence of diamagnetic localized gap states, some of which can be optically transformed into metastable paramagnetic states, but they are not specific enough as presently formulated to be compared with the ESR results in any detail.

In a recent series of papers concerning PL in chalcogenide glasses, Street and co-workers¹⁰ explained the PL temperature-dependence data and the shape of the PL excitation spectrum in terms of charged radiative recombination centers in the vicinity of which photon absorption is enhanced. Since the PL spectra in the crystalline counterpart of these glasses are quite similar to the glassy spectra, they concluded that an identical recombination center is involved in both phases, thereby restricting the recombination center to crystalline imperfections such as vacancies, interstitials, or stacking faults. All such defects involve broken bonds and broken or dangling As bonds were suggested as the charged recombination centers.

The most likely optically induced ESR centers (consistent with the conclusions of Sec. IV) would be holes on chalcogen dangling bond orbitals and electrons on As dangling bonds. However, since it is impossible on the basis of the ESR spectra to distinguish with certainty a hole in a dangling bond from a hole in a nonbonding orbital, (see Sec. IV A) one cannot rule out the possibility that while dangling bonds might be essential for the production of paramagnetic centers, the chalcogen center itself may consist of an electron missing from a normally filled nonbonding orbital.

More recently, Street and Mott¹⁸ have proposed a detailed model of localized gap states in chalcogenide glasses based on a two-electron pairing concept due to Anderson¹⁷ and on specific dangling bond configurations. A positively charged recombination center consists of an unoccupied dangling bond (D^+) which interacts with the nonbonding lone pair of a neighboring fully bonded chalcogen; the negatively charged center consists of a doubly occupied dangling bond (D^-) which forms a valence-band-like lone pair. The optically induced, metastable ESR centers (D^0) are explained by Street and Mott as the trapping of free electrons or holes by these charged centers. This model considers only one specific type of defect which can be unoccupied (D^+), singly occupied (D^0), or

doubly occupied (D^-), while it is now obvious that the observed ESR spectra in As_2Se_3 and As_2S_3 require two rather specific types of D^0 , one on a chalcogen and one on an As atom. It is also unclear how the model relates to amorphous As where there is no conclusive evidence for the existence of nonbonding p -type lone-pair wave functions and yet we have observed an optically induced metastable paramagnetic state.

Emin⁵⁶ has proposed a semiquantitative explanation of the optically induced experimental effects as well as dc transport properties in terms of an intrinsic small polaron model. The fundamental hypothesis of this model states that it is dynamically possible and energetically favorable for a carrier to form a *small polaron*, i.e., a state in which the atomic deformation produced by the charge carrier-lattice interaction self-traps the carrier. Reduced carrier mobility caused by disorder is thought to enhance the likelihood of small polaron formation. In Emin's model the general features of the luminescence, induced absorption and induced ESR in chalcogenide glasses are explained in terms of electronlike polarons in levels below the conduction band and holelike polarons above the valence band.

Economou, Ngai, and Reinecke²⁰ have recently described an approach in which the structural disorder modes which manifest themselves in several nonelectronic properties of glasses (such as the linear T dependence of the specific heat) also play a central role in determining the electronic states in the gap of amorphous semiconductors. This model calculation considers the influence of the two-level structural disorder modes (referred to by these authors as local rearrangement modes) on the electronic bonding states of the glass through either a Coulombic or a covalent interaction. The calculation predicts the mid-gap pinning of the Fermi energy, the pairing of localized electrons within the energy gap, as originally proposed by Anderson, and the general existence of optically produced paramagnetic states which are more prevalent in glasses with a "soft" structure.

VI. CONCLUDING REMARKS

As stated previously, while the optically induced localized paramagnetic states discussed here represent a nonequilibrium condition in the chalcogenide glasses, they do serve as highly sensitive probes of the local structural environment. In this respect, they provide information similar to that provided by ESR studies of paramagnetic centers produced in oxide glasses by radiation damage or doping with paramagnetic impurities. However, the optically induced nature of the centers in the

chalcogenide glasses and their intimate association with the radiative recombination process greatly enhance their usefulness as an experimental probe of the localized electronic states in these amorphous semiconductors. Information concerning local bonding configurations, extent of localization, possible defect structures, restrictions on the parentage of the optically induced states, and the concentration or density of these states can all be inferred from the optically induced ESR spectra presented here. While the information provided is not sufficient to generate a detailed description of the localized states and their role in such optical phenomena as photoluminescence, it does place meaningful restrictions upon the models proposed to explain these phenomena. The study of these optically induced paramagnetic states constitutes a powerful new technique which has provided valuable insights not accessible by other techniques concerning localized gap states

in amorphous semiconductors. It is believed that the continued study of the temperature and composition dependence of the optical and resonance phenomena associated with the optically induced states will yield substantial contributions to our still incomplete understanding of the role of lone-pair or nonbonding orbitals in the unique photo-electronic (PL and photoconductivity) and photo-structural effects observed in chalcogenide glasses.

ACKNOWLEDGMENTS

The authors gratefully acknowledge E. A. Davis, D. Emin, D. L. Mitchell, N. F. Mott, K. L. Ngai, T. L. Reinecke, and R. A. Street for many helpful discussions. We also wish to thank G. Pfister and W. A. LaCourse for supplying samples and E. J. Friebele and C. L. Marquardt for the use of their ESR apparatus.

-
- ¹M. H. Cohen, H. Fritzsche, and S. R. Ovshinsky, *Phys. Rev. Lett.* **22**, 1065 (1969).
- ²E. A. Davis and N. F. Mott, *Philos. Mag.* **22**, 903 (1970).
- ³H. Fritzsche, *J. Non-Cryst. Solids* **6**, 49 (1971).
- ⁴N. F. Mott and E. A. Davis, *Electronic Processes in Non-Crystalline Materials* (Clarendon, Oxford, 1971).
- ⁵H. Fritzsche, in *Electronic and Structural Properties of Amorphous Semiconductors*, edited by P. G. LeComber and J. Mort (Academic, New York, 1973), p. 55.
- ⁶H. Fritzsche, in *Amorphous and Liquid Semiconductors*, edited by J. Tauc (Plenum, New York, 1974), p. 221.
- ⁷J. Tauc, in *Amorphous and Liquid Semiconductors*, edited by J. Tauc (Plenum, New York, 1973), p. 159.
- ⁸B. T. Kolomiets, T. N. Mamontova, and A. A. Babaev, *J. Non-Cryst. Solids* **4**, 289 (1970).
- ⁹K. Weiser, *J. Non-Cryst. Solids* **8-10**, 922 (1972).
- ¹⁰R. A. Street, T. M. Searle, and I. G. Austin, *J. Phys. C* **6**, 1830 (1973); *Philos. Mag.* **30**, 1181 (1974); *ibid.* **29**, 1157 (1974).
- ¹¹J. Cernogora, F. Mollet, and C. Benoit à la Guillaume, *Phys. Status Solidi A* **15**, 401 (1973).
- ¹²S. G. Bishop and D. L. Mitchell, *Phys. Rev. B* **8**, 5696 (1973).
- ¹³S. C. Agarwal, *Phys. Rev. B* **7**, 685 (1973).
- ¹⁴A. E. Owen and J. W. Robertson, *J. Non-Cryst. Solids* **2**, 40 (1970).
- ¹⁵W. E. Spear and P. G. LeComber, *J. Non-Cryst. Solids* **8-10**, 727 (1972).
- ¹⁶F. J. DiSalvo, A. Menth, J. V. Waszczak, and J. Tauc, *Phys. Rev. B* **6**, 4574 (1972).
- ¹⁷P. W. Anderson, *Phys. Rev. Lett.* **34**, 953 (1975).
- ¹⁸R. A. Street and N. F. Mott, *Phys. Rev. Lett.* **35**, 1293 (1975).
- ¹⁹N. F. Mott, E. A. Davis, and R. A. Street, *Philos. Mag.* **32**, 961 (1975).
- ²⁰E. N. Economou, K. L. Ngai, and T. L. Reinecke, in *Linear and Nonlinear Electron Transport in Solids*, edited by J. T. Devreese and V. E. van Doren (Plenum, New York, 1976), p. 595.
- ²¹S. G. Bishop, U. Strom, and P. C. Taylor, *Phys. Rev. Lett.* **34**, 1346 (1975).
- ²²S. G. Bishop, U. Strom, and P. C. Taylor, *Phys. Rev. Lett.* **36**, 543 (1976).
- ²³S. G. Bishop, U. Strom, and P. C. Taylor, *Solid State Commun.* **18**, 573 (1976).
- ²⁴F. Stern, in *Solid State Physics*, edited by F. Seitz and D. Turnbull (Academic, New York, 1963), Vol. **15**, p. 378.
- ²⁵P. C. Taylor, H. M. Kriz, and J. F. Baugher, *Chem. Rev.* **75**, 203 (1975).
- ²⁶G. E. Pake, *Paramagnetic Resonance* (Benjamin, New York, 1962), p. 67.
- ²⁷T. H. DiStefano and D. E. Eastman, *Phys. Rev. Lett.* **27**, 1560 (1971).
- ²⁸N. J. Shevchik, M. Cardona, and J. Tejada, *Phys. Rev. B* **8**, 2833 (1973).
- ²⁹H. Ibach and J. E. Rowe, *Phys. Rev. B* **10**, 710 (1974).
- ³⁰S. G. Bishop and N. J. Shevchik, *Phys. Rev. B* **12**, 1567 (1975).
- ³¹D. L. Griscom, *J. Non-Cryst. Solids* **13**, 251 (1973/74).
- ³²J. W. H. Schreurs, *J. Chem. Phys.* **47**, 818 (1967).
- ³³The value of λ used for oxygen is that appropriate to neutral oxygen. A value of λ for the O^- ion might be more appropriate for the oxide glasses, but this value only differs from that for neutral oxygen by about 30%. [D. L. Griscom, P. C. Taylor, D. A. Ware and P. J. Bray, *J. Chem. Phys.* **48**, 5158 (1968).] This refinement may be neglected in view of the accuracy of the present calculations.
- ³⁴G. W. Charles, *J. Opt. Soc. Am.* **58**, 275 (1968).
- ³⁵D. L. Griscom, in *Proceedings of the Exeter Summer School on Defects in Solids* (Plenum, New York, to be published).
- ³⁶P. C. Taylor, U. Strom, and S. G. Bishop (unpublished).
- ³⁷C. M. Hurd and P. Coodin, *Phys. Chem. Solids* **20**, 523

- (1966).
- ³⁸P. W. Atkins and M. C. R. Symons, *The Structure of Inorganic Radicals* (American Elsevier, Amsterdam, 1967).
- ³⁹P. B. Ayscough, *Electron Spin Resonance in Chemistry* (Methuen, London, 1967).
- ⁴⁰A. M. Portis, *Phys. Rev.* **91**, 1071 (1953).
- ⁴¹J. S. Hyde, *Phys. Rev.* **119**, 1492 (1960).
- ⁴²In Portis's original formulation of Eq. (7) T_1^2 is replaced by $T_1 T_2$ because the microwave field is considered to interact with spins precessing in the frequency interval T_1^{-1} whereas Hyde's formulation considers that the microwave field interacts only with spins precessing in the frequency interval H_1 .
- ⁴³M. Kastner, D. Adler, and H. Fritzsche, *Phys. Rev. Lett.* **37**, 1504 (1976).
- ⁴⁴J. S. Berkes, S. W. Ing, Jr., and W. J. Hillegas, *J. Appl. Phys.* **42**, 4908 (1971).
- ⁴⁵J. P. DeNeufville, S. C. Moss, and S. R. Ovshinsky, *J. Non-Cryst. Solids* **13**, 191 (1974).
- ⁴⁶K. Tanaka, *Appl. Phys. Lett.* **26**, 243 (1975).
- ⁴⁷K. Tanaka, *AIP Conf. Proc.* **31**, 148 (1976).
- ⁴⁸S. G. Bishop and U. Strom, in *Optical Properties of Highly Transparent Solids*, edited by S. S. Mitra and B. Bendow (Plenum, New York, 1975), p. 317.
- ⁴⁹B. T. Kolomiets, T. N. Mamontova, and V. A. Vassilyev, in *Proceedings of the Sixth International Conference on Liquid and Amorphous Semiconductors*, edited by B. T. Kolomiets (Nauka, Leningrad, 1975), p. 227; and private communication.
- ⁵⁰S. G. Bishop, U. Strom, and P. C. Taylor, *Proceedings of the International Conference on the Physics of Semiconductors*, Rome, Italy, 30 Aug–3 Sept. 1976 (unpublished).
- ⁵¹S. R. Ovshinsky and K. Sapru, *Proceedings of the Fifth International Conference on Amorphous and Liquid Semiconductors*, edited by J. Stuke and W. Brenig (Taylor and Francis, London, 1974).
- ⁵²S. C. Agarwal and H. Fritzsche, *Phys. Rev. B* **10**, 4351 (1975).
- ⁵³S. R. Ovshinsky, *Phys. Rev. Lett.* **36**, 1469 (1976).
- ⁵⁴D. Engemann and R. Fischer, *Proceedings of the Fifth International Conference on Amorphous and Liquid Semiconductors*, edited by J. Stuke and W. Brenig (Taylor and Francis, London, 1974), p. 947.
- ⁵⁵S. G. Bishop, U. Strom, and P. C. Taylor, in Ref. 47, p. 16.
- ⁵⁶D. Emin (unpublished); and private communication.